Experimental pressure versus temperature isochoric – isoplethic curves for n-pentane – dimethyl ether, n-pentane – dimethyl ether – polybutadiene and n-pentane – dimethyl ether – polybutadiene– hydrogen at high pressures

Matías Menossi, Juan M. Milanesio, Andrés Ciolino, Séverine Camy, Marcelo S. Zabaloy

HAL Id: hal-02640554

https://hal.science/hal-02640554

Submitted on 28 May 2020

This is an author's version published in: http://oatao.univ-toulouse.fr/25857

Experimental pressure versus temperature isochoric – isoplethic curves for *n*-pentane – dimethyl ether, *n*-pentane – dimethyl ether – polybutadiene and *n*-pentane – dimethyl ether – polybutadiene–hydrogen at high pressures

Matías Menossi [a], Juan M. Milanesio [a,*], Andrés Ciolino [b], Séverine Camy [c],
Marcelo S. Zabaloy [b]

[a] *Instituto de investigación y desarrollo en ingeniería de Procesos y Química Aplicada – IPQA, Facultad de Ciencias Exactas Físicas y Naturales, Universidad Nacional de Córdoba, CONICET, Av. Vélez Sarsfield 1611, Ciudad Universitaria, X5016GCA, Córdoba, Argentina*
[b] *Planta Piloto de Ingeniería Química – PLAPIQUI, Universidad Nacional del Sur (UNS), CONICET, Camino La Carrindanga Km 7 – CC 717, Bahía Blanca, Argentina*
[c] *Laboratoire de Génie Chimique, Université de Toulouse, CNRS, INPT, UPS, Toulouse, France*

G R A P H I C A L   A B S T R A C T
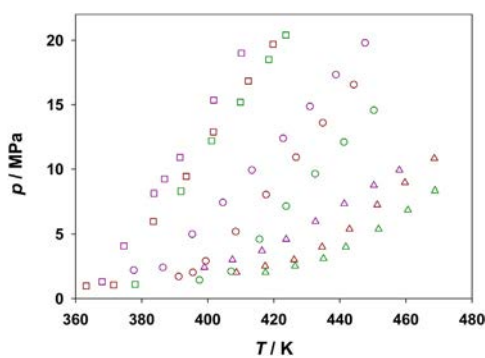
A B S T R A C T

Loci of isochoric - isoplethic experimental phase equilibrium data, were determined for the binary mixture dimethyl ether (DME) + *n*-pentane (C_5); the ternary mixture: DME + C_5 + polybutadiene (PB); and the quaternary mixture DME + C_5 + PB + hydrogen (H_2). Binary experiments were performed at varying overall density (ρ) and varying quantity of C_5. Ternary experiments were performed at varying ρ and varying relative quantities of each light solvent. In the case of quaternary mixtures, the mass fraction of polymer was kept constant, and the amount of H_2 and ρ were varied. The experimental data obtained for binary and ternary mixtures were correlated using the Perturbed-Chain Statistical Associating Fluid Theory (PC-SAFT) equation of state (EoS).

* Corresponding author.
E-mail address: juan.milanesio@unc.edu.ar (J.M. Milanesio).

1. Introduction

The hydrogenation of polybutadienes (PBs) of narrow molecular weight distribution results in polymers similar to linear low-density polyethylenes (LLDPEs) with polydispersity index (PD) close to unity.

The hydrogenation reaction of heavy polymers is conventionally carried out dissolving it in an organic solvent, such as toluene or cyclohexane, and injecting hydrogen (H_2) into the reactor, which implies a reaction pressure significantly greater than the atmospheric pressure. Two fluid phases are present in the reactor during the hydrogenation course, because of the low solubility of H_2 in the polymer-containing liquid phase.

Changing the conventionally used solvents for other light solvents, at relatively low pressures, will not change the phase scenario inside the reactor, i.e., the unsaturated polymer will remain dissolved in the liquid phase, and the hydrogen (H_2) will remain almost pure in the vapor phase. This situation implies a H_2 mass transfer rate limitation due to the presence of the interphase between the liquid and the vapor phases inside the reactor.

Alternatively, the H_2 and the heavy unsaturated compound can be made to coexist in a single homogeneous fluid phase if a supercritical solvent (or solvent mixture) is added to the system. This fluid homogeneity should imply an increase in the reaction rate due to the absence of a fluid-fluid interphase, and to the higher concentration achieved for one of the reactants (H_2) in the (only) fluid phase where the reaction takes place. Piqueras et al. [1] showed that the hydrogenation of sunflower oil, using platinum as catalyst and supercritical propane as solvent, can be up to 12 times faster than the conventional hydrogenation.

The use of a light solvent as a component of a solvent mixture may speed up the hydrogenation, even in the presence of two-fluid phases, due to the potential improvement of the transport properties.

The conventional hydrogenation of PB (presence of two fluid phases) can be accomplished using heterogeneous or homogeneous catalysts [2]. When using heterogeneous catalysts, the PB hydrogenation process involves high conversions with minimum chain scission [2], but the process is relatively slow and it needs an elevated 'catalyst/double bonds' mole ratio, due to the "poisoning" of the catalyst caused by impurities present in the reaction media [2–7]. The use of homogeneous catalysts for hydrogenating PB implies higher reaction times to achieve complete hydrogenation, and also the need for higher temperatures and pressures, in comparison to the PB hydrogenation using heterogeneous catalysts.

The high asymmetry of the reactive PB + H_2 mixture, which is due to the large difference in molecular size between the H_2 and PB molecules, implies a high immiscibility level in the absence of the compressed solvent or compressed solvent mixture. Thus, to hydrogenate the PB in a single fluid phase, the solvent (or solvent mixture) should be able to simultaneously dissolve the PB and the H_2 at the initial stage of the reaction. The subsystems 'solvent mixture + H_2', 'PB + solvent mixture', and 'PB + solvent mixture + H2′ should be homogenous at the conditions of temperature, pressure and PB concentration, at which the hydrogenation is to be carried out.

In this context, one of the main goals of the present work is to experimentally find conditions of homogeneity for binary dimethyl ether (DME) + n-pentane (C_5) solvent mixtures, ternary DME + C_5 + PB mixtures and quaternary mixtures obtained by adding the H_2. C_5 and DME have been previously identified as possible components of the solvent mixture for the PB hydrogenation in a single fluid phase [2,8]. Experimental data have also been obtained in this work for the pure compounds carbon dioxide (CO_2) and toluene, in order to validate, in part, the experimental apparatus. This work complements information available in previous

works related to the search for convenient conditions to carry out the hydrogenation of PB under fluid homogeneity conditions [2,8]. One of the differences with our previous works is the incorporation of the unsaturated polymer together with the H_2 to emulate the phase scenario of the mixture at the beginning of the hydrogenation reaction.

To experimentally find, in this work, phase boundaries for the binary, ternary and quaternary mixtures, the isochoric/isoplethic method was used. The isochoric/isoplethic method has been used by several authors to measure dew and bubble points and densities (PVT information) of fluids [9–13].

The final long-term goal of the modeling part is to describe the phase scenario of the reactive mixture at different conditions. Computational problems arise due to the great asymmetry of these systems, mainly related to the addition of H_2. Therefore, only binary and ternary mixtures (that include the polymer) could be modeled in this work.

2. Experimental

2.1. Materials

Grupo Linde Gas Argentina S.A. (Pilar, Buenos Aires, Argentina) supplied CO2 with a purity level greater than 99.9% (GC) (124-38-9 CAS number). Toluene 99.5% wt% (GC) (108-88-3 CAS number) was provided by Biopack (Zárate, Buenos Aires, Argentina). DME (115-10-6 CAS number), with a purity level greater than 99%, (GC) was purchased from Sigma Aldrich (Sheboygan, Wisconsin, USA). Ciccarelli (San Lorenzo, Santa Fe, Argentina) provided the C_5 (109-66-0 CAS number) greater than 97.0% wt% pure. H_2 (1333-74-0 CAS number) was provided by Grupo Linde Gas Argentina with a purity level greater than 97% (GC).

Table 1 summarizes the source and purity information for such chemicals. Table 2 provides the values of some relevant physical properties for the light components used in our experiments.

Polybutadiene was synthesized in our lab by high-vacuum anionic polymerization [15]. The obtained PB number-average molecular weight (Mn) is 23.5 kg/mol. The PB weight-average molecular weight (Mw) is 30.9 kg/mol and the PB PD index is 1.31. The average molecular weights were determined by size exclusion chromatography (SEC). The SEC system is equipped with a Waters pump (515 HPLC Pump, Refractive Index Detector 2414, Rheodyne 7725i Injector) and with four PLGel columns of 0.00000005,

Table 1
Description of chemical used in this work.

Chemical name	Source	Purity
hydrogen (H_2)	Grupo linde	0.97*
n-pentane (C_5)	Ciccarelli	>0.97**
dimethyl ether (DME)	Sigma Aldrich	>0.99*
carbon dioxide (CO_2)	Grupo linde	>0.999*
toluene	Biopack	0.995**

* Mole fraction.
** wt %.

Table 2
Properties of pure solvents [14].

Compound	M/kg mol^{-1}	T_c/ K	p_c/MPa	ρ_c/kg m^{-3}	T_b/K
hydrogen (H_2)	0.0020	33.19	1.31	31	20.39
n-pentane (C_5)	0.0722	469.70	3.37	231	309.22
dimethyl ether (DME)	0.0461	400.10	5.37	271	248.31
carbon dioxide (CO_2)	0.0440	304.21	7.38	468	194.67*
toluene	0.0921	591.14	4.11	292	383.78

M: Molecular weight, T_C: Critical temperature, p_C: Critical pressure, ρ_c: Critical density, T_b: normal boiling point.
* Normal sublimation point.

Table 3
Characteristics of PB used in this work.

M_w (kg/mol)	M_n (kg/mol)	PD index (M_w/M_n)	1,2-vinyl content (%)
30.9	23.5	1.31	14.7

0.000001, 0.00001 and 0.0001 m porosity, respectively. The solvent employed was toluene at 298 K with a flow rate of 1.66×10^{-8} m^3/s. The injection volume was 2×10^{-4} m^3 and the molecular weights of the polymers were estimated following the standard calibration procedure using monodisperse polystyrene (PS) samples and the corresponding Mark-Houwink coefficients for each polymer in toluene (PB: K' = 1.6×10^{-5} m^3 kg^{-1}; α = 0.765; PS: K' = 1.2×10^{-5} m^3 kg^{-1}; α = 0.710) [16].

PB is an unsaturated polymer formed from the polymerization of 1,3-butadiene. Depending on the reaction conditions, 1,3-butadiene can polymerize generating 1,4-cis and 1,4-trans or 1,2-vinyl configurations in the polymer chain. The PB used in this work shows 14.7% of 1,2-vinyl configuration according to proton nuclear magnetic resonance spectrum (^{1}H-NMR). The ^{1}H-NMR spectrum (Appendix A) was obtained with a Bruker advance II apparatus (400 Hz frequency) at room temperature, using deuterated chloroform (CDCl$_3$) as the solvent. Chemical shifts were expressed in ppm downfield from tetramethyl silane (TMS) as internal standard. The molecular structure of the polymer is presented in Appendix A indicating the protons corresponding to its double bonds: 1,2 (vinyl) and 1,4 (cis and trans) [17]. Table 3 shows all the characteristics of the PB used in this work.

2.2. Phase equilibria apparatus

Fig. 1 shows the experimental setup. The heart of the apparatus is an in-house constant volume cell which was built on the basis of equipment described in the literature [12]. The constant-volume cell is housed in an adapted gas chromatography (GC) oven (Shimadzu GC-R1A (2) to assure temperature homogeneity. A PID controller (IBEST, Model TCN4M24R) connected to a thermocouple (inside the GC oven) is used to keep the oven temperature at the desired set value.

Fig. 2 shows a schematic diagram of the equilibrium cell. The cell (7) is a stainless-steel tube (closed at both ends) with a nominal diameter of 0.0127 m and a wall thickness of 2.5×10^{-3} m. The inner volume of the cell is $1.893 \times 10^{-5} \pm 8.000 \times 10^{-8}$ m^3. This value was determined by completely filling, at ambient conditions, the dry cell with a liquid of known density, which was injected into the cell by using a regular syringe, whose weight loss made possible to measure the mass of loaded liquid. This mass was next converted to volume by using the known density value.

The cell pressure is measured to ± 0.41 MPa with a Bourdon-type manometer (1) (see Fig. 2) (Winter PFP series, maximum pressure: 27.46 MPa). The temperature of the fluid system located inside the cell is measured with a K-type thermocouple (4) (see Fig. 2) independent from the temperature control system.

The K-type thermocouple (4) was calibrated by using an industrial temperature calibrator (Isotech, model: Fast-Cal ISO 9000, range: 303–623 K, uncertainty = ± 0.3 K). The uncertainty in the recorded temperature values is estimated to be in the order of ± 0.5 K. The manometer (1) was calibrated against a hydraulic dead-weight tester (Fluke, model: P3124-3, uncertainty = ± 0.008%). The experimental setup does not include devices for stirring the fluid system inside the cell. The cell has no sight windows.

To determine the amount of solvent loaded into the cell, a TA302 Ohaus Traveller ($0.3 \pm 1 \times 10^{-5}$ kg) electronic precision scale was used, for both, liquid and gaseous components (i.e. those who are gaseous compounds under ambient conditions). The measurements were compared with a R31P3 Ranger Ohaus ($3 \pm 1 \times 10^{-4}$ kg) precision scale. For PB masses, a AX124/E Adventurer Ohaus precision balance (accuracy $0.12 \pm 1 \times 10^{-7}$ kg) was used.

The experimental window of conditions is determined by two physical limits, one is the degradation temperature of the PTFE tape (about 473 K) used to tighten the cell caps, and the second is the bursting pressure of the cell, at which the cell rupture will occur (approximately 25 MPa).

2.3. Methodology

In a typical binary, ternary or quaternary experiment, the constant-volume cell is loaded with a known amount of each compound of the mixture. Next, the temperature of the system is set, and after equilibrium is reached, the pressure is measured and recorded, together with the values of temperature, global density and global composition. The equilibrium situation may correspond to a heterogeneous fluid system inside the cell or to a homogeneous fluid. Equilibrium is considered to be reached when the
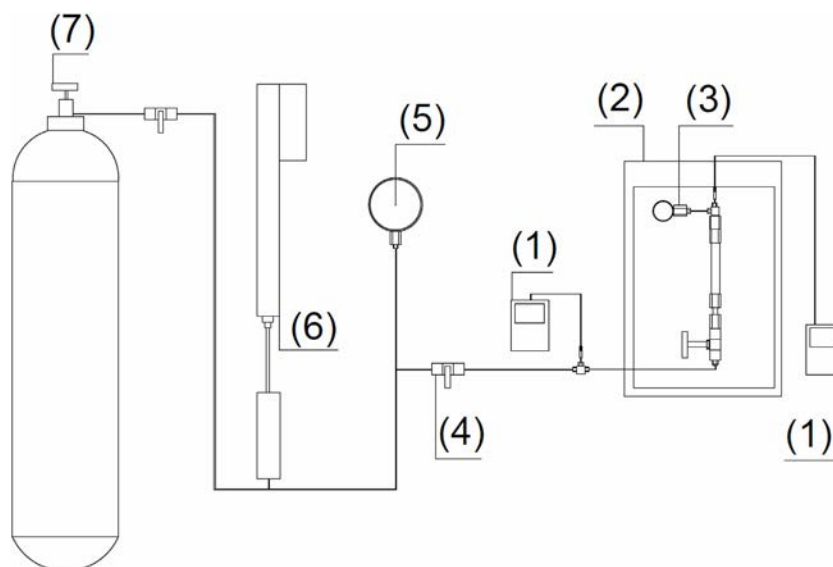
Fig. 1. Experimental setup: (1) Temperature indicators. (2) Gas chromatography oven. (3) Constant volume cell. (4) Valve. (5) Manometer. (6) High-pressure syringe. (7) H$_2$ tube.
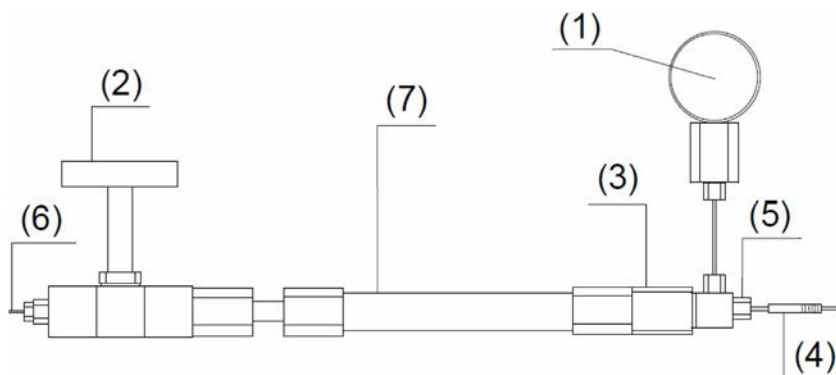
Fig. 2. Constant volume cell setup: (1) Manometer. (2) Valve for loading/discharging the cell. (3) High-pressure union (removed to load PB). (4) Thermocouple. (5) Thermocouple fitting (removed to load liquid solvents). (6) Charging line for gaseous solvents. (7) Body of the constant volume cell.

cell pressure remains constant for at least 1800 s (indeed the constancy of the cell temperature is also required). The measurement is repeated at other temperatures, in the desired temperature range. The recorded pressure versus temperature experimental points constitute an isoplethic (constant overall composition) and isochoric (constant overall density) phase equilibrium locus or trajectory. A discontinuous change in slope in this pressure versus temperature trajectory implies a phase transition, i.e., a change in the phase scenario inside the cell. For the sake of conciseness, we often refer to the mentioned trajectories simply as "isochores". Pure compound isochores are obtained in the same way that multicomponent isochores except that only a single component is loaded into the cell.

For the binary, ternary or quaternary mixtures, the total mass of chemicals loaded into the cell, would be set so that the overall density (ρ) value would correspond to a system having, at high enough temperature, a liquid nature, or a liquid-liquid nature, when possible. In the case of the pure compounds, the overall density value always corresponded to a homogeneous liquid nature at high enough temperature. The uncertainties in the mixture composition were estimated through a very conservative propagation of error analysis [18], for all systems studied.

2.3.1. Cell loading procedure

At laboratory ambient conditions (atmospheric pressure and approximately 298 K) DME, H_2 and CO_2 are gases and C_5 and toluene are liquids (see normal boiling point values in Table 2). The PB used is a highly viscous liquid. PB is loaded inside the cell by using a laboratory spoon whose weight loss equals the amount of loaded PB. A given pure liquid component is charged by employing a regular syringe, and the loaded mass is obtained from the weight loss of the syringe. A given pure gaseous component (except H_2) is loaded with the help of an auxiliary cell (AC) and the charged amount is obtained from the weight loss of the AC. H_2 is charged into the cell by using a high-pressure syringe (6) (see Fig. 1). As explained in detail in the supplementary material, the uncertainty in the global mass fraction of H_2 is not reported in this paper since it cannot be reliably estimated. This makes our data for the system DME + C_5 + PB + H_2 have a semiquantitative nature. Thus, our experimental data for H_2-containing systems are useful mainly to identify trends in the phase behavior of the mixture. The supplementary material provides detailed information on the procedures for loading the different components into the cell.

Once the cell is loaded, it is placed in the oven (2) (see Fig. 1). Next, the temperature of the system is set. After the equilibrium is reached, no observable changes in pressure are detected at constant temperature. Both, temperature and pressure are recorded.

3. Modeling

The phase behavior of the studied systems was modeled using the well-known Perturbed-Chain Statistical Associating Fluid Theory [20] (PC-SAFT) equation of state (EoS). The commercial software SimuLis Thermodynamics (PROSIM SA, Labege, FRANCE) was used for most computations involving the PC-SAFT model.

The PC-SAFT-EoS was used for computing phase envelopes, isolated bubble pressures, critical points and isoplethic/isochoric pressure vs temperature trajectories. The PC-SAFT model is written as a sum of contributions to the residual Helmholtz energy at given temperature, volume and composition, i.e., a "hard spheres" term, a "chain" term and a "dispersion" term. The pure-compound parameters of the PC-SAFT-EoS are the segment diameter σ, the number of segments m, and the dispersive energy ε/k (where k is the Boltzmann constant). For mixtures, the PC-SAFT-EoS provides an interaction parameter k_{ij} which appears in the combining rule that defines the crossed dispersive energy parameter ε_{ij} as follows:

$$\varepsilon_{ij} = \sqrt{\varepsilon_i \varepsilon_j} \left(1 - k_{ij}\right) \tag{1}$$

For computing, using the PC-SAFT-EoS, pure-compound isoplethic-isochoric pressure vs temperature trajectories, the selected task was the liquid-vapor flash computation at set temperature and set global molar volume. The output of this computation is the pressure of the system, the number of phases, and the relative amount of each phase at equilibrium, i.e., the vaporization ratio.

For binary or ternary mixtures, the point of an isochore where the P vs T slope has a discontinuous change is, for the systems and conditions studied in this work, the bubble point of the mixture at the set isochore global composition and set global density (which equals the liquid phase density at the bubble point). A set of bubble points obtained from several isochores, all having the same global composition; describe part of an isoplethic phase boundary (phase envelope, see, e.g., Fig. 5). Analogously, a set of dew points obtained from several isochores describe the remaining part of the isoplethic phase boundary. Bubble points estimated in this work from our ternary experimental isochoric/isoplethic data (Table 11) were used here to fit the k_{ij} parameters of the PC-SAFT-EoS. The details are available in the supplementary material. Simulis Thermodynamics was used to compute the bubble points and, when possible, the dew points, at given temperature, composition (=global composition) and model parameter values.

Once the optimum values of the binary interaction parameters k_{ij} were determined, a flash algorithm was used to compute complete binary and ternary isoplethic-isochoric pressure vs temperature trajectories, at constant overall composition and constant overall density. In this case, a flash algorithm at set temperature, pressure and global composition was the chosen task. This task has

Table 4
Pressure as a function of temperature at constant overall density for pure CO_2. Experimental data obtained in this work. T = absolute temperature; p = absolute pressure; ρ = overall density.

$\rho = 404 \pm 8\,\mathrm{kg\,m^{-3}}$			$\rho = 489 \pm 9\,\mathrm{kg\,m^{-3}}$			$\rho = 638 \pm 11\,\mathrm{kg\,m^{-3}}$		
T/K	p/MPa	Phase condition*	T/K	p/MPa	Phase condition*	T/K	p/MPa	Phase condition*
299.0	6.17 ± 0.48	LV	310.3	8.15 ± 0.58	SC	289.7	5.09 ± 0.43	LV
310.0	7.75 ± 0.56	SC	320.3	10.02 ± 0.67	SC	294.4	5.78 ± 0.47	LV
320.0	9.23 ± 0.63	SC	330.3	12.00 ± 0.76	SC	299.7	6.57 ± 0.50	LV
330.5	10.91 ± 0.71	SC	340.3	13.87 ± 0.85	SC	309.1	8.54 ± 0.60	SC
340.5	12.39 ± 0.78	SC	350.3	15.75 ± 0.94	SC	314.3	10.12 ± 0.67	SC
350.7	13.77 ± 0.85	SC	359.6	17.43 ± 1.02	SC	319.6	11.60 ± 0.75	SC
360.6	15.25 ± 0.92	SC	368.7	19.10 ± 1.10	SC	330.7	14.86 ± 0.90	SC
370.0	16.44 ± 0.97	SC				340.3	17.82 ± 1.04	SC
						344.3	19.00 ± 1.10	SC

u(T) = ±0.5 K. u is the standard uncertainty in the measurement.
* LV = liquid-vapor. SC = supercritical.

Table 5
Pressure as a function of temperature at constant overall density for pure toluene. Experimental data obtained in this work. T = absolute temperature; p = absolute pressure; ρ = overall density.

$\rho = 775 \pm 12\,\mathrm{kg\,m^{-3}}$			$\rho = 765 \pm 12\,\mathrm{kg\,m^{-3}}$			$\rho = 731 \pm 11\,\mathrm{kg\,m^{-3}}$		
T/K	p/MPa	Phase condition*	T/K	p/MPa	Phase condition*	T/K	p/MPa	Phase condition*
397.1	7.46 ± 0.55	L	399.4	2.52 ± 0.41	L	432.4	2.03 ± 0.41	L
399.1	9.43 ± 0.64	L	404.5	5.48 ± 0.45	L	438.5	5.48 ± 0.45	L
402.8	11.50 ± 0.74	L	409.2	8.25 ± 0.59	L	442.4	7.85 ± 0.57	L
407.5	14.37 ± 0.88	L	413.4	10.42 ± 0.69	L	448.3	10.91 ± 0.71	L
410.4	16.04 ± 0.96	L	418.4	12.89 ± 0.81	L	453.3	13.28 ± 0.83	L
413.7	17.92 ± 1.05	L	423.4	15.85 ± 0.95	L	458.5	15.65 ± 0.94	L
416.2	20.31 ± 1.16	L	428.3	20.46 ± 1.17	L	463.3	19.46 ± 1.12	L

u(T) = ±0.5 K. u is the standard uncertainty in the measurement.
* L = liquid.

the global density (or molar volume) as one of its output variables. This flash calculation was an inner loop of a loop whose iteration variable was the pressure, which was changed until the computed overall density matched the experimental overall density.

In the case of ternary mixtures, the dew point algorithm of Simulis Thermodynamics was unable to calculate the dew pressure at given temperature and composition of the mixture.

4. results and discussion

4.1. Phase transitions in pure compounds

To partially validate the experimental technique, isochores were measured for the pure compounds CO_2 and toluene, at two-phase and single-phase conditions; and compared with data from the NIST Chemistry Webbook [19].

Tables 4 and 5 present the raw experimental isoplethic/isochoric pressure vs temperature data obtained in this work for the pure compounds CO_2 and toluene, respectively.

Fig. 3 shows the evolution of pressure as a function of temperature for pure CO_2 at constant overall mass densities of $638 \pm 11\,\mathrm{kg \cdot m^{-3}}$, $489 \pm 9\,\mathrm{kg \cdot m^{-3}}$ and $404 \pm 8\,\mathrm{kg \cdot m^{-3}}$. Our experimental data (Table 4) are the red circles, triangles and squares in Fig. 3, which includes the uncertainty bars for our experimental pressure. The pure CO_2 vapor-liquid equilibrium curve obtained from Ref. [19] is indicated as a continuous blue line. Part of our data are biphasic (vapor-liquid, lower temperatures) and part are monophasic (liquid or vapor, higher temperatures). When going from lower to higher temperatures, the two-phase to one-phase transition would be indicated by a discontinuity in the isochore slope. Such discontinuity is clearly noticed in Fig. 3 for the highest density (i.e., 638 kg m⁻³) but it is not for the two lower densities, since their values (489 ± 9 and $404 \pm 8\,\mathrm{kg\,m^{-3}}$) are close, in relative terms, to the critical density of pure CO_2 ($\rho_{c,CO2} = 468\,\mathrm{kg\,m^{-3}}$,
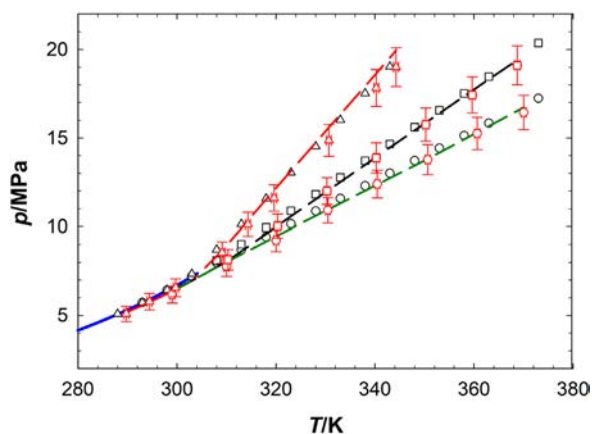
Fig. 3. Pressure vs temperature at constant overall density (ρ) for pure CO_2. Experimental data:
(△) ρ = 638 kg m⁻³ (this work, Table 4).
(□) ρ = 489 kg m⁻³ (this work, Table 4).
(○) ρ = 404 kg m⁻³ (this work, Table 4).
(△) ρ = 638 kg m⁻³ (Ref. [19]).
(□) ρ = 489 kg m⁻³ (Ref. [19]).
(○): ρ = 404 kg m⁻³ (Ref. [19]).
(— —): Calculated isochore at ρ = 638 kg m⁻³ (Model: PC-SAFT).
(— —): Calculated isochore at ρ = 489 kg m⁻³ (Model: PC-SAFT).
(— —): Calculated isochore at ρ = 404 kg m⁻³ (Model: PC-SAFT).
Pure compound vapor-liquid equilibrium curve: (—) CO_2 [19].

Table 2). The critical temperature (T_c) and critical density (ρ_c) of pure CO_2 are 304.21 K and 468 kg m⁻³ respectively (Table 2). The transition from vapor-liquid heterogeneity to liquid homogeneity should happen at approximately 302 K in Fig. 3 at a density of 489 kg m⁻³ and to vapor homogeneity at approximately 300 K at a density 404 kg m⁻³. The black triangles, squares and circles in Fig. 3 are data corresponding to the CO_2 isochores given by Ref. [19]. They

Table 6
PC-SAFT parameters for pure compounds.

	C_5 [*]	DME [20]	CO_2 [20]	Toluene [20]	PB [25]
m	2.720	2.307	2.073	2.815	1312.941
σ (m)x10^{-9}	3.753	3.253	2.785	3.717	3.389
ε/k (K)	229.9	211.1	169.2	285.7	269.3

[*] Parameter values for C_5 taken from the software database (Simulis Thermodynamics 2015).

Fig. 4. Pressure vs temperature at constant overall density (ρ) for pure toluene.
Experimental data:
($\triangle$) $\rho = 775$ kg m^{-3} (this work, Table 5).
($\square$) $\rho = 765$ kg m^{-3} (this work, Table 5).
($\bigcirc$) $\rho = 731$ kg m^{-3} (this work, Table 5).
($\bigcirc$): $\rho = 775$ kg m^{-3} (Ref. [19]).
($\triangle$) $\rho = 765$ kg m^{-3} (Ref. [19]).
($\square$) $\rho = 731$ kg m^{-3} (Ref. [19]).
(— —): Calculated isochore at $\rho = 775$ kg m^{-3} (Model: PC-SAFT).
(— —): Calculated isochore at $\rho = 765$ kg m^{-3} (Model: PC-SAFT).
(— —): Calculated isochore at $\rho = 731$ kg m^{-3} (Model: PC-SAFT).
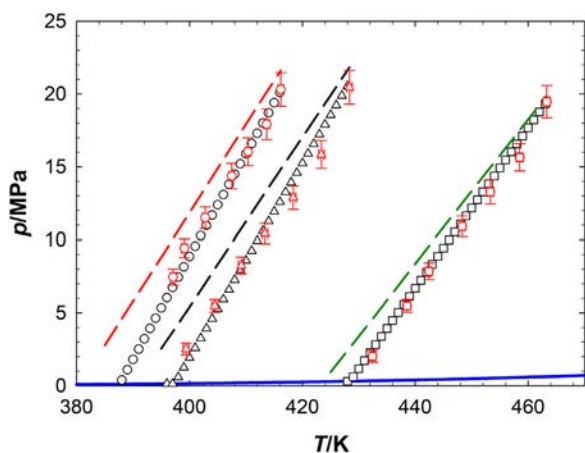Pure compound vapor-liquid equilibrium curve: (—) toluene [19].

show a good level of agreement with our data. Our experimental CO_2 data (Table 4) are also consistent with the predicted PC-SAFT isochores (dashed lines in Fig. 3). The PC-SAFT parameter values used for the pure compounds are reported in Table 6.

In the case of toluene, three constant mass densities were considered: 775 ± 12, 765 ± 12 and 731 ± 11 kg·m^{-3}. In all cases, the densities are much higher than the critical density of toluene ($\rho_{c,toluene} = 292$ kg m^{-3}, Table 2). Thus, at a temperature less than T_c, there will be a vapor-liquid to liquid transition, in the isochore.

Table 5 presents our experimental isoplethic/isochoric data for pure toluene. They are shown as red circles, triangles and squares, from higher to lower densities, in Fig. 4. The blue line is the pure toluene vapor-liquid equilibrium curve [19]. For this compound, our isochores only have monophasic (liquid) segments. The slopes of the isochores in the homogeneous region increase with increasing overall density. The black triangles, squares and circles in Fig. 4 are data from Ref. [19]. They roughly agree with our data. The slopes of the isochoric segments predicted by the PC-SAFT-EoS differ from those of our experimental data and of the NIST [19] data. The relative error in pressure, given by the EoS, decreases with increasing temperature.

4.2. Phase transitions in the binary mixture ($DME + C_5$)

Table 7 and Figs. 5 and 6 show, for the binary system $DME + C_5$, our experimental isoplethic/isochoric data for different combinations of global density and global composition. Fig. 5 shows three isochores of $X_{C5} \approx 0.4$, and Fig. 6 presents two sets of isochores: one of $X_{C5} \approx 0.6$ and the other of $X_{C5} \approx 0.75$.
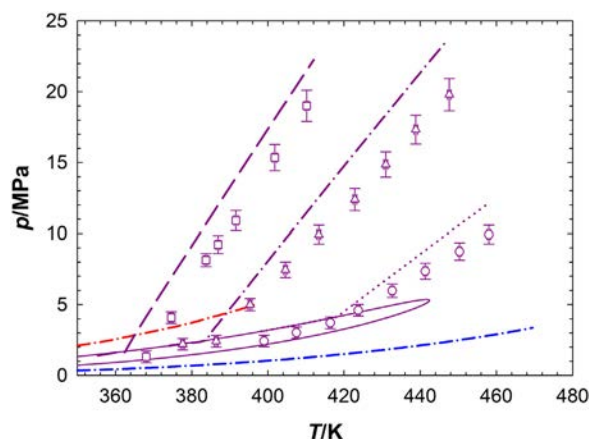
Fig. 5. Pressure vs temperature at constant overall composition (X_{C5}) and constant overall density (ρ) for the system $DME + C_5$.
Experimental data (this work, Table 7):
($\square$) $\rho = 539$ kg m^{-3}, $X_{C5} = 0.409$.
($\triangle$) $\rho = 497$ kg m^{-3}, $X_{C5} = 0.400$.
($\bigcirc$) $\rho = 401$ kg m^{-3}, $X_{C5} = 0.390$.
Computed isochoric/isoplethic loci (Model: PC-SAFT, $k_{DME,C5} = 0.019$):
(— —) $\rho = 539$ kg m^{-3}, $X_{C5} = 0.409$.
(— · —) $\rho = 497$ kg m^{-3}, $X_{C5} = 0.400$.
(...) $\rho = 401$ kg m^{-3}, $X_{C5} = 0.390$.
Computed phase envelope (Model: PC-SAFT, $k_{DME,C5} = 0.019$):
(—) $X_{C5} = 0.400$.
Pure compound vapor-liquid equilibrium curves: (— · —): DME [21].
(— · —): C_5 [19].
X_{C5}: C_5 mole fraction.
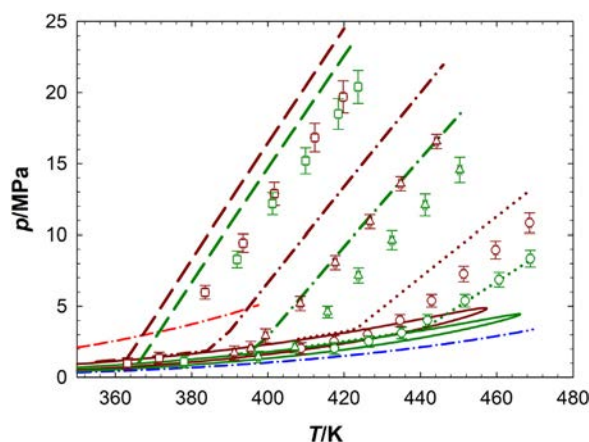
Fig. 6. Pressure vs temperature at constant overall composition (X_{C5}) and constant overall density (ρ) for the system $DME + C_5$.
Experimental data (this work, Table 7):
($\square$) $\rho = 539$ kg m^{-3}, $X_{C5} = 0.605$.
($\triangle$) $\rho = 502$ kg m^{-3}, $X_{C5} = 0.593$.
($\bigcirc$) $\rho = 423$ kg m^{-3}, $X_{C5} = 0.613$.
($\square$) $\rho = 544$ kg m^{-3}, $X_{C5} = 0.764$.
($\triangle$) $\rho = 491$ kg m^{-3}, $X_{C5} = 0.755$.
($\bigcirc$) $\rho = 391$ kg m^{-3}, $X_{C5} = 0.767$.
Computed isochoric/isoplethic loci (Model: PC-SAFT, $k_{DME,C5} = 0.019$):
(— —) $\rho = 539$ kg m^{-3}, $X_{C5} = 0.605$.
(— · —) $\rho = 502$ kg m^{-3}, $X_{C5} = 0.593$.
(...) $\rho = 423$ kg m^{-3}, $X_{C5} = 0.613$.
(— —) $\rho = 544$ kg m^{-3}, $X_{C5} = 0.764$.
(— · —) $\rho = 491$ kg m^{-3}, $X_{C5} = 0.755$.
(...) $\rho = 391$ kg m^{-3}, $X_{C5} = 0.767$.
Computed phase envelopes (Model: PC-SAFT, $k_{DME,C5} = 0.019$):
(—): $X_{C5} = 0.600$; (—): $X_{C5} = 0.750$.
Pure compound vapor-liquid equilibrium curves: (— · —): DME [21].
(— · —): C_5 [19]. X_{C5}: C_5 mole fraction.

Table 7

Experimental equilibrium pressure as a function of temperature at constant overall composition (X_{C5}) and constant overall density (ρ) for the C_5 + DME system. Experimental data obtained in this work. T = absolute temperature; p = absolute pressure; X_{C5} = overall C_5 mole fraction.

$X_{C5} = 0.765 \pm 0.013$			$X_{C5} = 0.390 \pm 0.012$			$X_{C5} = 0.400 \pm 0.010$		
$\rho = 520 \pm 10 \,\mathrm{kg\,m^{-3}}$			$\rho = 401 \pm 9 \,\mathrm{kg\,m^{-3}}$			$\rho = 497 \pm 9 \,\mathrm{kg\,m^{-3}}$		
T/K	p/MPa	Phase condition*	T/K	p/MPa	Phase condition*	T/K	p/MPa	Phase condition*
383.9	1.54 ± 0.41	LV	399.0	2.42 ± 0.41	LV	377.6	2.20 ± 0.41	LV
392.0	4.99 ± 0.43	L	407.5	3.02 ± 0.41	LV	386.4	2.41 ± 0.41	LV
405.1	8.74 ± 0.61	L	416.4	3.71 ± 0.41	LV	395.3	4.99 ± 0.43	L
414.1	12.29 ± 0.78	L	423.8	4.59 ± 0.41	L	404.6	7.46 ± 0.55	L
421.4	14.86 ± 0.90	L	432.6	5.98 ± 0.47	L	413.4	9.93 ± 0.66	L
428.5	17.62 ± 1.03	L	441.3	7.36 ± 0.54	L	422.9	12.39 ± 0.78	L
			450.3	8.74 ± 0.61	SC	430.9	14.86 ± 0.90	L
			458.0	9.93 ± 0.66	SC	438.8	17.33 ± 1.02	L
						447.6	19.79 ± 1.14	SC

$X_{C5} = 0.409 \pm 0.010$			$X_{C5} = 0.613 \pm 0.014$			$X_{C5} = 0.593 \pm 0.012$		
$\rho = 539 \pm 10 \,\mathrm{kg\,m^{-3}}$			$\rho = 423 \pm 9 \,\mathrm{kg\,m^{-3}}$			$\rho = 502 \pm 10 \,\mathrm{kg\,m^{-3}}$		
T/K	p/MPa	Phase condition*	T/K	p/MPa	Phase condition*	T/K	p/MPa	Phase condition*
368.0	1.31 ± 0.41	LV	408.7	2.03 ± 0.41	LV	391.2	1.71 ± 0.41	LV
374.6	4.08 ± 0.41	L	417.4	2.52 ± 0.41	LV	395.5	2.03 ± 0.41	LV
383.7	8.14 ± 0.46	L	426.2	3.02 ± 0.41	LV	399.4	2.92 ± 0.41	L
386.9	9.23 ± 0.63	L	434.6	4.00 ± 0.41	L	408.5	5.19 ± 0.44	L
391.6	10.91 ± 0.71	L	442.9	5.39 ± 0.45	L	417.7	8.07 ± 0.58	L
401.8	15.35 ± 0.93	L	451.3	7.27 ± 0.54	L	426.8	10.92 ± 0.71	L
410.2	19.01 ± 1.10	L	459.7	8.95 ± 0.62	SC	434.8	13.59 ± 0.84	L
			486.6	10.83 ± 0.71	SC	444.2	16.56 ± 0.98	L

$X_{C5} = 0.605 \pm 0.011$			$X_{C5} = 0.767 \pm 0.018$			$X_{C5} = 0.755 \pm 0.014$			$X_{C5} = 0.764 \pm 0.013$		
$\rho = 539 \pm 10 \,\mathrm{kg\,m^{-3}}$			$\rho = 391 \pm 10 \,\mathrm{kg\,m^{-3}}$			$\rho = 491 \pm 10 \,\mathrm{kg\,m^{-3}}$			$\rho = 544 \pm 10 \,\mathrm{kg\,m^{-3}}$		
T/K	p/MPa	Phase condition*	T/K	p/MPa	Phase condition*	T/K	p/MPa	Phase condition*	T/K	p/MPa	Phase condition*
363.2	0.98 ± 0.41	LV	417.4	2.03 ± 0.41	LV	397.5	1.44 ± 0.41	LV	378.0	1.10 ± 0.41	LV
371.5	1.35 ± 0.41	LV	426.4	2.52 ± 0.41	LV	407.1	2.11 ± 0.41	LV	391.9	8.30 ± 0.59	L
383.5	5.98 ± 0.48	L	435.0	3.11 ± 0.41	LV	415.7	4.59 ± 0.41	L	401.2	12.20 ± 0.77	L
393.5	9.43 ± 0.64	L	441.8	4.00 ± 0.41	L	423.8	7.16 ± 0.53	L	409.9	15.20 ± 0.92	L
401.7	12.89 ± 0.81	L	451.7	5.39 ± 0.45	L	432.5	9.63 ± 0.65	L	418.5	18.50 ± 1.08	L
412.3	16.83 ± 1.00	L	460.6	6.86 ± 0.52	L	441.2	12.10 ± 0.77	L	423.7	20.40 ± 1.17	L
419.8	19.70 ± 1.13	L	468.8	8.35 ± 0.59	SC	450.3	14.56 ± 0.89	L			

u(T) = ±0.5 K. u is the standard uncertainty in the measurement.

* Estimated phase condition. *L = liquid. LV = liquid-vapor. SC = supercritical.

Table 8

Bubble points[a] for the C_5 + DME binary mixture. T = absolute temperature; p = absolute pressure; X_{C5} = overall C_5 mole fraction; ρ = overall density (= saturated liquid density).

X_{C5}	$\rho/\mathrm{kg\,m^{-3}}$	T/K	p/MPa
0.390 ± 0.012	401 ± 9	416.4	3.71 ± 0.41
0.400 ± 0.010	497 ± 10	386.4	2.41 ± 0.41
0.613 ± 0.014	423 ± 9	426.2	3.02 ± 0.41
0.593 ± 0.012	502 ± 10	395.5	2.03 ± 0.41
0.605 ± 0.011	539 ± 10	371.5	1.35 ± 0.41
0.767 ± 0.018	391 ± 10	435.0	3.11 ± 0.41
0.755 ± 0.014	491 ± 10	407.1	2.11 ± 0.41

u(T) = ±0.5 K. u is the standard uncertainty in the measurement.

a Estimated from the isoplethic/isochoric experimental data of Table 7.

Table 9

Computed[a] critical pressures (p_c), critical temperatures (T_c) and critical densities (ρ_c) at set composition (X_{C5}) for the binary system C_5+DME ($k_{C5,DME}$ = 0.019). X_{C5} = C_5 mole fraction.

X_{C5}	T_c/K	p_c/MPa	$\rho_c/\mathrm{kg\,m^{-3}}$
0.4	443.8	5.27	245
0.6	457.2	4.81	238
0.75	466.1	4.45	232

a Model: PC-SAFT-EoS. Pure compound parameters in Table 6.

In Figs. 5 and 6, for each one of the isochores, there are two distinguishable segments, i.e., a (regarded as) biphasic slightly curved low temperature segment, and a high temperature quasi linear segment, where there is a single phase, i.e., a liquid phase, inside the cell. The transition point is considered to be a bubble point at the given global composition. The isochore global density is also the saturated liquid density at such bubble point. The bubble points estimated from Figs. 5 and 6 for the DME + C_5 binary system are reported in Table 8. The estimation is made by finding the intersection point between the isochore low temperature and high temperature segments.

Figs. 5 and 6 also show the phase envelopes (thin solid lines), of same global composition than the experimental data, calculated with the PC-SAFT-EoS. The model overpredicts the slopes of the liquid segments, except for the isochore of lowest density [ρ = 391 kg m³ and X_{C5} = 0.767, Fig. 6] where we see a fairly good agreement between model and experimental data. The PC-SAFT error in the calculated pressure can be as high as 4 MPa for the denser binary mixtures.

Notice that in Figs. 5 and 6 the pure compound vapor-liquid equilibrium curves are shown as well.

We computed, using the algorithms of Ref. [22], for $k_{DME,C5}$ = 0.019, the DME + C_5 mixture critical pressure, critical temperature and critical mass density at the compositions of Figs. 5 and 6. The results are shown in Table 9.

As it can be seen, the isochore overall mass density in Figs. 5 and 6 is, in all cases, higher than the corresponding computed

Table 10

Experimental equilibrium pressure as a function of temperature at constant overall composition (W_{C_5}, W_{PB}) and constant overall density (ρ) for the C_5+DME+PB system. Experimental data obtained in this work. T = absolute temperature; p = absolute pressure; W_{C_5} = overall C_5 mass fraction; W_{PB} = overall PB mass fraction.

$W_{C_5} = 0.495 \pm 0.014$ $W_{PB} = 0.053 \pm 0.001$ $\rho = 385 \pm 9\,\mathrm{kg\,m^{-3}}$

T/K	p/MPa	Phase condition*
394.0	2.52 ± 0.41	LV
402.6	3.21 ± 0.41	LV
411.1	3.90 ± 0.41	LV
420.4	4.60 ± 0.41	LV
428.1	5.29 ± 0.44	L
436.0	6.08 ± 0.48	L
444.5	7.36 ± 0.54	L or SC
452.0	8.64 ± 0.60	L or SC
461.2	10.02 ± 0.67	L or SC

$W_{C_5} = 0.491 \pm 0.010$ $W_{PB} = 0.049 \pm 0.001$ $\rho = 506 \pm 10\,\mathrm{kg\,m^{-3}}$

T/K	p/MPa	Phase condition*
374.7	1.54 ± 0.41	LV
383.5	2.33 ± 0.41	LV
394.1	5.48 ± 0.45	L
402.8	7.95 ± 0.57	L
412.0	10.42 ± 0.69	L
420.2	12.89 ± 0.81	L
428.9	15.35 ± 0.93	L
436.9	17.82 ± 1.04	L

$W_{C_5} = 0.485 \pm 0.010$ $W_{PB} = 0.050 \pm 0.001$ $\rho = 534 \pm 10\,\mathrm{kg\,m^{-3}}$

T/K	p/MPa	Phase condition*
362.5	1.83 ± 0.41	LV
372.2	3.61 ± 0.41	L
380.8	6.57 ± 0.50	L
389.1	9.53 ± 0.65	L
398.7	12.49 ± 0.79	L
407.5	15.55 ± 0.94	L
416.5	18.51 ± 1.08	L

$W_{C_5} = 0.673 \pm 0.013$ $W_{PB} = 0.048 \pm 0.001$ $\rho = 416 \pm 9\,\mathrm{kg\,m^{-3}}$

T/K	p/MPa	Phase condition*
403.3	2.03 ± 0.41	LV
412.7	2.62 ± 0.41	LV
420.9	3.11 ± 0.41	LV
429.0	3.90 ± 0.41	LV
437.9	4.99 ± 0.43	L
445.9	6.08 ± 0.48	L or SC
453.6	7.26 ± 0.54	L or SC
462.2	8.54 ± 0.60	L or SC

$W_{C_5} = 0.651 \pm 0.010$ $W_{PB} = 0.050 \pm 0.001$ $\rho = 511 \pm 10\,\mathrm{kg\,m^{-3}}$

T/K	p/MPa	Phase condition*
390.2	1.91 ± 0.41	LV
394.6	1.93 ± 0.41	LV
403.7	5.48 ± 0.45	L
410.7	7.85 ± 0.57	L
420.9	10.32 ± 0.68	L
429.8	12.89 ± 0.81	L
438.1	15.45 ± 0.93	L
447.0	17.92 ± 1.05	L or SC

$W_{C_5} = 0.673 \pm 0.010$ $W_{PB} = 0.050 \pm 0.001$ $\rho = 534 \pm 10\,\mathrm{kg\,m^{-3}}$

T/K	p/MPa	Phase condition*
366.2	1.31 ± 0.41	LV
371.8	1.54 ± 0.41	LV
380.3	4.00 ± 0.41	L
389.9	6.96 ± 0.52	L
398.5	9.92 ± 0.67	L
407.7	12.89 ± 0.81	L
416.6	15.85 ± 0.95	L
425.5	18.81 ± 1.09	L

$W_{C_5} = 0.775 \pm 0.013$ $W_{PB} = 0.050 \pm 0.001$ $\rho = 400 \pm 9\,\mathrm{kg\,m^{-3}}$

T/K	p/MPa	Phase condition*
412.3	2.03 ± 0.41	LV
419.7	2.52 ± 0.41	LV
428.6	3.02 ± 0.41	LV
437.0	3.81 ± 0.41	L
445.3	4.89 ± 0.42	L
453.4	5.98 ± 0.48	L or SC
461.8	7.26 ± 0.54	L or SC

$W_{C_5} = 0.781 \pm 0.011$ $W_{PB} = 0.050 \pm 0.001$ $\rho = 500 \pm 10\,\mathrm{kg\,m^{-3}}$

T/K	p/MPa	Phase condition*
394.1	1.54 ± 0.41	LV
401.5	2.03 ± 0.41	LV
410.7	4.00 ± 0.41	L
419.5	6.96 ± 0.52	L
427.0	9.43 ± 0.64	L
437.0	12.39 ± 0.78	L
444.4	14.86 ± 0.90	L
452.5	17.33 ± 1.02	L or SC

$W_{C_5} = 0.789 \pm 0.010$ $W_{PB} = 0.050 \pm 0.001$ $\rho = 534 \pm 10\,\mathrm{kg\,m^{-3}}$

T/K	p/MPa	Phase condition*
392.1	5.48 ± 0.45	L
400.3	8.64 ± 0.60	L
409.0	11.70 ± 0.75	L
418.9	14.76 ± 0.90	L
425.9	16.93 ± 1.00	L

$u(T) = \pm 0.5\,\mathrm{K}$. u is the standard uncertainty in the measurement.

* Estimated phase condition. *L = liquid. LV = liquid-vapor. SC = supercritical.

DME + C_5 mixture critical mass density (Table 9). This implies a liquid nature for the isochore homogeneous segment, and, in principle a P vs. T slope of the homogeneous segment greater than the slope of the isochore vapor-liquid segment. In all cases, the higher the density, the lower the break point temperature. Also, the break point temperature decreases with the increase in the light component global mole fraction, at constant composition of the mixture.

Outcalt and Lemmon [23] obtained compressed liquid densities for the system DME + C_5 in an isoplethic-isothermal-isobaric densimeter. At a composition $X_{C_5} = 0.765$, at a pressure of P = 5 MPa and a temperature of 390 K they report a density of $\rho = 520\,\mathrm{kg\,m^{-3}}$ for the mixture. In our work, with the same overall density ($\rho = 520\,\mathrm{kg\,m^{-3}}$), a C_5 mole fraction of $X_{C_5} = 0.787$ and a temperature of 392 K, the experimental pressure is P = 4.99 MPa. As it can be seen, there is a good quantitative agreement. The difference can be attributed to the slight difference between compositions.

Considering bubble pressures, using a variable-volume phase equilibrium cell Outcalt and Lemmon [24] reported a bubble pressure value P = 1.48 MPa at T = 370 K and $X_{C_5} = 0.608$. The closest bubble point obtained in this work (from isochoric data) has coordinates T = 371.5 K, $X_{C_5} = 0.605$ and P = 1.35 MPa (Table 8). The difference between both bubble pressure values lies within the estimated uncertainty of our value (± 0.41 MPa).

4.3. Phase transitions in ternary mixture (PB + DME + C_5)

Nine isochores were measured for the ternary mixture PB + DME + C_5. They were obtained at varying overall densities and varying overall composition of the DME + C_5 solvent mixture, while keeping the mass fraction of the polymer practically constant, as shown in Table 10. Notice that for ternary and quaternary mixtures, the composition is given in the weight fraction scale. The curves are shown in Figs. 7 and 8. Their behavior is analogous to the one described for the binary system DME + C_5. The bubble points estimated from Figs. 7 and 8 are reported in Table 11. Such bubble points were used to estimate the PC-SAFT-EoS interaction parameters k_{DME,C_5}, k_{PB,C_5} and $k_{DME,PB}$ reported in Table 12. The k_{DME,C_5} value was used to calculate phase envelopes and the isochoric trajectories in the binary mixture, as it was shown in Figs. 5 and 6.

Fig. 7 shows three isochores whose C_5 mass fraction is, approximately, $W_{C_5} = 0.5$, while in Fig. 8 the isochores have $W_{C_5} = 0.67$ and $W_{C_5} = 0.78$. Again we see that the higher the overall density,
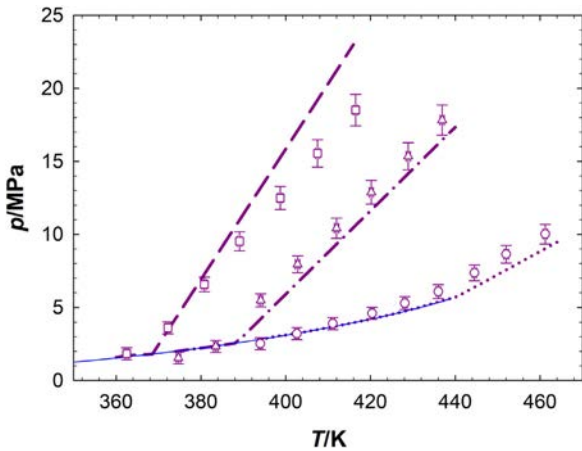
Fig. 7. Pressure vs temperature at constant overall composition (W_{C_5}, W_{PB}) and constant overall density (ρ) for the system DME + C_5 + PB.
Experimental data (this work, Table 10):
($\square$) $\rho = 534$ kg m^{-3}, $W_{C_5} = 0.485$; $W_{PB} = 0.050$.
($\triangle$) $\rho = 506$ kg m^{-3}, $W_{C_5} = 0.491$; $W_{PB} = 0.049$.
($\bigcirc$) $\rho = 385$ kg m^{-3}, $W_{C_5} = 0.495$; $W_{PB} = 0.053$.
Computed isochoric/isoplethic loci (Model: PC-SAFT, $k_{DME,C_5} = 0.019$, $k_{C_5,PB} = 0.159$, $k_{DME,PB} = -0.052$):
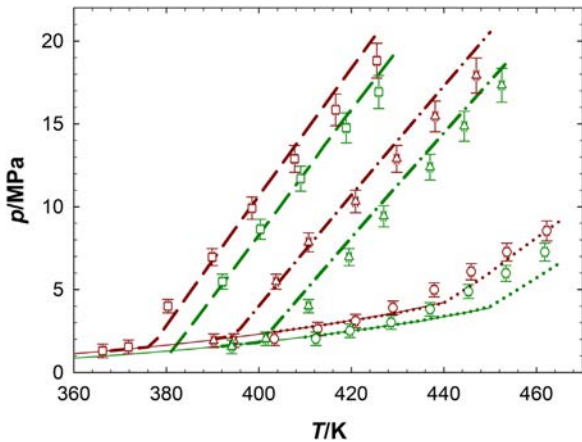(—— ——) $\rho = 534$ kg m^{-3}, $W_{C_5} = 0.485$; $W_{PB} = 0.050$.
(—— · ——) $\rho = 506$ kg m^{-3}, $W_{C_5} = 0.491$; $W_{PB} = 0.049$.
(...) $\rho = 385$ kg m^{-3}, $W_{C_5} = 0.495$; $W_{PB} = 0.053$.
Computed bubble points (Model: PC-SAFT, $k_{DME,C_5} = 0.019$, $k_{C_5,PB} = 0.159$, $k_{DME,PB} = -0.052$):
(——): $W_{C_5} = 0.490$; $W_{PB} = 0.050$.
W_{C_5}: C_5 mass fraction. W_{PB}: PB mass fraction.

Fig. 8. Pressure vs temperature at constant overall composition (W_{C_5}, W_{PB}) and constant overall density (ρ) for the system DME + C_5 + PB.
Experimental data (this work, Table 10):
($\square$) $\rho = 534$ kg m^{-3}, $W_{C_5} = 0.673$; $W_{PB} = 0.050$.
($\triangle$) $\rho = 511$ kg m^{-3}, $W_{C_5} = 0.651$; $W_{PB} = 0.050$.
($\bigcirc$) $\rho = 416$ kg m^{-3}, $W_{C_5} = 0.673$; $W_{PB} = 0.048$.
($\square$) $\rho = 534$ kg m^{-3}, $W_{C_5} = 0.789$; $W_{PB} = 0.050$.
($\triangle$) $\rho = 500$ kg m^{-3}, $W_{C_5} = 0.781$; $W_{PB} = 0.050$.
($\bigcirc$) $\rho = 400$ kg m^{-3}, $W_{C_5} = 0.775$; $W_{PB} = 0.050$.
Computed isochoric/isoplethic loci (Model: PC-SAFT, $k_{DME,C_5} = 0.019$, $k_{C_5,PB} = 0.159$, $k_{DME,PB} = -0.052$):
(—— ——) $\rho = 534$ kg m^{-3}, $W_{C_5} = 0.673$; $W_{PB} = 0.050$.
(—— · ——) $\rho = 511$ kg m^{-3}, $W_{C_5} = 0.651$; $W_{PB} = 0.050$.
(...) $\rho = 416$ kg m^{-3}, $W_{C_5} = 0.673$; $W_{PB} = 0.048$.
(—— ——) $\rho = 534$ kg m^{-3}, $W_{C_5} = 0.789$; $W_{PB} = 0.050$.
(—— · ——) $\rho = 500$ kg m^{-3}, $W_{C_5} = 0.781$; $W_{PB} = 0.050$.
(...) $\rho = 400$ kg m^{-3}, $W_{C_5} = 0.775$; $W_{PB} = 0.050$.
Computed bubble points (Model: PC-SAFT, $k_{DME,C_5} = 0.019$, $k_{C_5,PB} = 0.159$, $k_{DME,PB} = -0.052$):
(——): $W_{C_5} = 0.670$; $W_{PB} = 0.050$; (——): $W_{C_5} = 0.780$; $W_{PB} = 0.050$. W_{C_5}: C_5 mass fraction. W_{PB}: PB mass fraction.

Table 11
Bubble points[a] for the C_5 + DME + PB ternary mixture. T = absolute temperature; p = absolute pressure; W_{C_5} = overall C_5 mass fraction; W_{PB} = overall PB mass fraction; ρ = overall density (= saturated liquid density).

W_{C_5}	W_{PB}	ρ/kg m^{-3}	T/K	p/MPa
0.495 ± 0.014	0.053 ± 0.001	385 ± 9	420.4	4.60 ± 0.41
0.491 ± 0.010	0.049 ± 0.001	506 ± 10	383.5	2.33 ± 0.41
0.673 ± 0.013	0.048 ± 0.001	416 ± 9	429.0	3.90 ± 0.41
0.651 ± 0.010	0.050 ± 0.001	511 ± 10	394.6	1.93 ± 0.41
0.673 ± 0.010	0.050 ± 0.001	534 ± 10	371.8	1.54 ± 0.41
0.775 ± 0.013	0.050 ± 0.001	400 ± 9	428.6	3.02 ± 0.41
0.781 ± 0.011	0.050 ± 0.001	500 ± 10	401.5	2.03 ± 0.41

$u(T) = \pm 0.5$ K. u is the standard uncertainty in the measurement.
[a] Estimated from the isoplethic/isochoric experimental data of Table 10.

Table 12
Binary interaction parameters.

Component i	Component j	k_{ij}
C_5	DME	0.019
C_5	PB	0.159
DME	PB	−0.052

the lower the bubble temperature. For example, for the isochore at $\rho = 506$ kg m^{-3}, $W_{C_5} = 0.491$ and $W_{PB} = 0.049$, the bubble point coordinates are: 383.5 K and 2.33 MPa, while, for the isochore at $\rho = 385$ kg m^{-3}, $W_{C_5} = 0.495$ and $W_{PB} = 0.053$ the bubble point coordinates are: 420.4 K and 4.60 MPa. Also, steeper single-phase segments are observed for denser ternary mixtures.

Figs. 7 and 8 also show, as thin solid lines, computed loci of bubble points of same global composition than that of the experimental ternary data, calculated with the PC-SAFT-EoS. PC-SAFT parameters for the pure PB were taken from Yelash et al. [25] and are reported in Table 6. The complete phase envelopes could not be calculated by the Simulis Thermodynamics software because the dew point algorithm did not converge for the polymer containing mixtures. Fig. 7 shows that the PC-SAFT overpredicts the homogeneous segment slope for the heaviest mixture [$\rho = 534$ kg m^{-3} and $W_{C_5} = 0.485$]. In Fig. 8, the computed homogeneous-liquid-mixture segments show a fairly good agreement with the experimental data except for the lightest ternary mixtures [$\rho = 400$ kg m^{-3} and $W_{C_5} = 0.673$; and $\rho = 416$ kg m^{-3} and $W_{C_5} = 0.775$].

The data suggest that the addition of polymer to the binary solvent mixture increases the bubble pressure at a given composition and temperature. For instance, the bubble point measured for C_5 + DME at $X_{C_5} = 0.605$ (or $WC_5 = 0.71$), and at an overall density of $\rho = 539$ kg m^{-3} (see Table 8) has coordinates 371.5 K and 1.35 MPa. If part of the C_5 is replaced by PB while keeping the same overall density ($W_{C_5} = 0.673$, $W_{PB} = 0.05$ and $\rho = 534$ kg m^{-3}), the measured bubble point is 371.8 K and 1.54 MPa (Table 11), i.e., the bubble pressure is 0.2 MPa higher. A similar observation was also informed by Byun and Lee [26]. They measured bubble pressures in a high-pressure variable volume cell for the binary system CO_2 + decyl acrylate (DA) and for the ternary mixture CO_2 + DA + poly(DA). At a temperature of 353.15 K and at a DA mole fraction of $X_{DA} = 0.135$, the addition of 6 wt% of poly(DA) increases the bubble pressure from 15.47 MPa to 15.79 MPa.

4.4. Phase transitions in quaternary system: solvents + polymer + hydrogen (DME + C_5 + PB+H_2)

To properly emulate the initial reactive mixture for a potential single-phase high-pressure hydrogenation of PB, seven isochoric/isoplethic pressure vs temperature trajectories were measured, adding hydrogen to the ternary mixture DME + C_5 + PB. The experimental data are presented in Table 13. These data are semiquantitative in nature, due to the lack of estimates for the
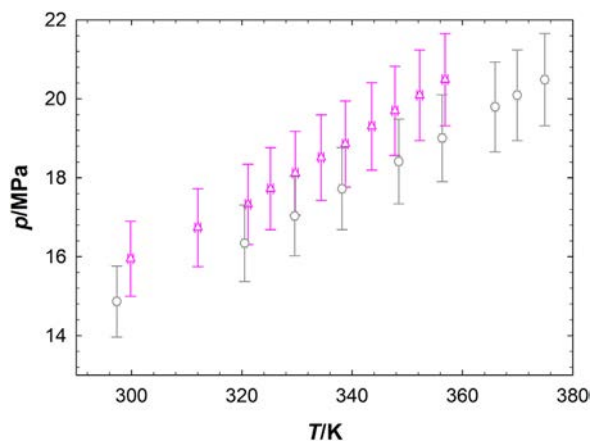
Table 13

Experimental equilibrium pressure as a function of temperature at constant overall composition (W_{C_5}, W_{PB}, W_{H_2}) and constant overall density (ρ) for the C_5 + DME + PB + H_2 system. Semiquantitative experimental data obtained in this work. T = absolute temperature; p = absolute pressure; W_{C_5} = overall C_5 mass fraction; W_{PB} = overall PB mass fraction; W_{H_2} = overall H_2 mass fraction.

W_{C_5} = 0.486 ± 0.013		W_{C_5} = 0.487 ± 0.015		W_{C_5} = 0.497 ± 0.018		W_{C_5} = 0.477 ± 0.015	
W_{DME} = 0.473 ± 0.013		W_{DME} = 0.472 ± 0.015		W_{DME} = 0.461 ± 0.018		W_{DME} = 0.477 ± 0.015	
W_{PB} = 0.030 ± 0.001		W_{PB} = 0.030 ± 0.001		W_{PB} = 0.030 ± 0.001		W_{PB} = 0.030 ± 0.001	
W_{H_2} = 0.011		W_{H_2} = 0.011		W_{H_2} = 0.012		W_{H_2} = 0.016	
ρ = 402 ± 23 kg m^{-3}		ρ = 347 ± 25 kg m^{-3}		ρ = 298 ± 26 kg m^{-3}		ρ = 354 ± 20 kg m^{-3}	
T/K	p/MPa	T/K	p/MPa	T/K	p/MPa	T/K	p/MPa
298.0	14.37 ± 0.88	298.7	12.49 ± 0.79	301.0	7.46 ± 0.55	299.6	15.85 ± 0.95
330.9	16.83 ± 1.00	330.8	14.56 ± 0.89	349.3	9.33 ± 0.64	321.1	17.52 ± 1.03
335.1	17.13 ± 1.01	340.0	15.25 ± 0.92	358.1	9.73 ± 0.66	325.5	17.92 ± 1.05
339.0	17.43 ± 1.03	348.7	15.95 ± 0.95	367.2	10.22 ± 0.68	330.5	18.36 ± 1.07
343.8	17.72 ± 1.04	358.5	16.73 ± 0.99	376.6	10.81 ± 0.71	334.9	18.81 ± 1.09
349.1	18.12 ± 1.06	367.3	17.62 ± 1.03	385.3	11.41 ± 0.74	339.4	19.30 ± 1.11
353.2	18.51 ± 1.08	375.6	18.51 ± 1.08	393.6	12.00 ± 0.77	344.0	19.74 ± 1.14
357.6	19.10 ± 1.11	384.7	19.50 ± 1.13	403.9	12.69 ± 0.80	348.8	20.19 ± 1.16
362.4	19.70 ± 1.13			412.9	13.38 ± 0.83	353.2	20.68 ± 1.18
366.5	20.19 ± 1.16			421.6	14.07 ± 0.86		
				430.3	14.86 ± 0.90		
				438.4	15.55 ± 0.93		
				447.0	16.34 ± 0.97		
				455.2	17.13 ± 1.01		

| W_{C_5} = 0.485 ± 0.018		W_{C_5} = 0.482 ± 0.018		W_{C_5} = 0.483 ± 0.019	
W_{DME} = 0.467 ± 0.018		W_{DME} = 0.464 ± 0.018		W_{DME} = 0.464 ± 0.019	
W_{PB} = 0.031 ± 0.001		W_{PB} = 0.031 ± 0.001		W_{PB} = 0.031 ± 0.001	
W_{H_2} = 0.017		W_{H_2} = 0.023		W_{H_2} = 0.022	
ρ = 294 ± 21 kg m^{-3}		ρ = 296 ± 18 kg m^{-3}		ρ = 285 ± 18 kg m^{-3}	
T/K	p/MPa	T/K	p/MPa	T/K	p/MPa
301.9	11.60 ± 0.75	299.8	15.95 ± 0.95	297.3	14.86 ± 0.90
330.1	13.28 ± 0.83	312.0	16.73 ± 0.99	320.5	16.34 ± 0.97
339.1	13.87 ± 0.85	321.1	17.33 ± 1.02	329.6	17.03 ± 1.01
348.4	14.37 ± 0.88	325.2	17.72 ± 1.04	338.2	17.72 ± 1.04
357.5	14.91 ± 0.90	329.7	18.12 ± 1.06	348.5	18.41 ± 1.07
366.8	15.70 ± 0.94	334.4	18.51 ± 1.08	356.3	19.00 ± 1.10
376.2	16.44 ± 0.98	338.8	18.86 ± 1.09	365.9	19.79 ± 1.14
385.3	17.13 ± 1.01	343.6	19.30 ± 1.11	369.9	20.09 ± 1.15
393.7	17.82 ± 1.04	347.8	19.70 ± 1.13	374.9	20.49 ± 1.17
403.0	18.61 ± 1.08	352.3	20.09 ± 1.15		
411.8	19.40 ± 1.12	356.8	20.49 ± 1.17		

u(T) = ±0.5 K. u is the standard uncertainty in the measurement.
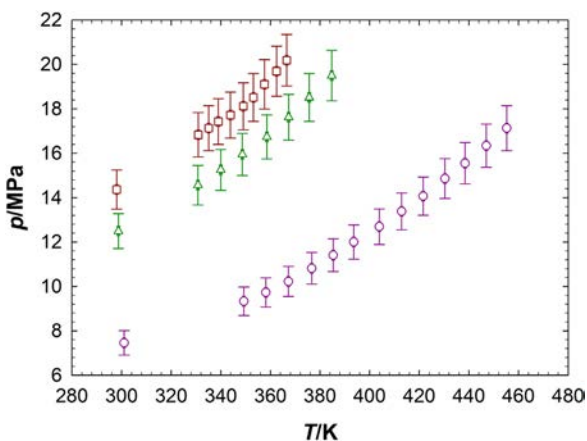
Fig. 9. Pressure vs temperature at constant overall composition (W_{C5}, W_{PB}, W_{H2}) and constant overall density (ρ) for the system DME + C_5 + PB + H_2. Semiquantitative experimental data (this work, Table 13):
($\square$) ρ = 402 kg m^{-3}, W_{C5} = 0.486; W_{PB} = 0.030; W_{H2} = 0.011.
($\triangle$) ρ = 347 kg m^{-3}, W_{C5} = 0.487; W_{PB} = 0.030; W_{H2} = 0.011.
($\bigcirc$) ρ = 298 kg m^{-3}, W_{C5} = 0.497; W_{PB} = 0.030; W_{H2} = 0.012.
W_{C5}: C_5 mass fraction. W_{PB}: PB mass fraction. W_{H2}: H_2 mass fraction.

Fig. 11. Pressure vs temperature at constant overall composition (W_{C5}, W_{PB}, W_{H2}) and constant overall density (ρ) for the system DME + C_5 + PB + H_2. Semiquantitative experimental data (this work, Table 13):
($\triangle$) ρ = 296 kg m^{-3}, W_{C5} = 0.482; W_{PB} = 0.031; W_{H2} = 0.023.
($\bigcirc$) ρ = 285 kg m^{-3}, W_{C5} = 0.483; W_{PB} = 0.031; W_{H2} = 0.022.
W_{C5}: C_5 mass fraction. W_{PB}: PB mass fraction. W_{H2}: H_2 mass fraction.
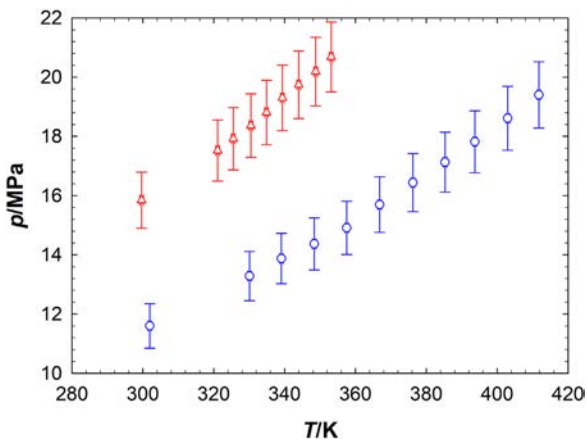
Fig. 10. Pressure vs temperature at constant overall composition (W_{C5}, W_{PB}, W_{H2}) and constant overall density (ρ) for the system DME + C_5 + PB + H_2. Semiquantitative experimental data (this work, Table 13):
($\triangle$) ρ = 354 kg m^{-3}, W_{C5} = 0.477; W_{PB} = 0.030; W_{H2} = 0.016.
($\bigcirc$) ρ = 294 kg m^{-3}, W_{C5} = 0.485; W_{PB} = 0.031; W_{H2} = 0.017.
W_{C5}: C_5 mass fraction. W_{PB}: PB mass fraction. W_{H2}: H_2 mass fraction.
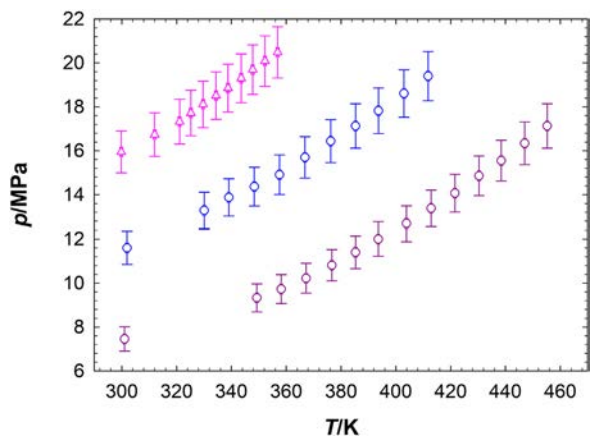
Fig. 12. Pressure vs temperature at constant overall composition (W_{C5}, W_{PB}, W_{H2}) and constant overall density (ρ) for the system DME + C_5 + PB + H_2. Semiquantitative experimental data (this work, Table 13):
($\triangle$) ρ = 296 kg m^{-3}, W_{C5} = 0.482; W_{PB} = 0.031; W_{H2} = 0.023.
($\bigcirc$) ρ = 294 kg m^{-3}, W_{C5} = 0.485; W_{PB} = 0.031; W_{H2} = 0.017.
($\bigcirc$) ρ = 298 kg m^{-3}, W_{C5} = 0.497; W_{PB} = 0.030; W_{H2} = 0.012.
W_{C5}: C_5 mass fraction. W_{PB}: PB mass fraction. W_{H2}: H_2 mass fraction.

uncertainty in the H_2 global mass fraction, as previously mentioned (see details in the Supplementary material).

Figs. 9–11 show isochores at different densities for quaternary mixtures. The hydrogen content increases when going from Figs. 9–11 ($W_{H2} \approx 0.010$ in Fig. 9, $W_{H2} \approx 0.015$ in Fig. 10 and $W_{H2} \approx 0.020$ in Fig. 11). The C_5 content of the mixture is approximately $W_{C5} = 0.48$ and the PB mass fraction is approximately 0.03 in all three figures. Clear slope discontinuities are not observed in Figs. 9–11. Hence, we find no evidence of phase transitions in our quaternary experimental data.

Regarding the modeling, the experimental data in Table 13 could not be fitted using the PC-SAFT-EoS. The flashes for the quaternary system could not be calculated by using the mentioned commercial software.

In view of these limitations, we computed isochores at global compositions and densities resulting from the removal of H_2 from the mixtures whose compositions and densities are reported in Table 13 and Figs. 9–11. The temperature ranges of the computations where the same than those of the isochores in Figs. 9–11. The thus specified (calculated) isochores were found to be biphasic

within the whole set temperature range. For all computed points, both phases were found to be quite far from being incipient, so that it would not be expected that the addition of H_2 would induce a transition to a homogeneity situation. This is consistent with the lack of clearly noticeable slope discontinuities in the data of Figs. 9–11. This suggests that no experimental datum in such figures corresponds to a single-phase system. Global densities higher than the studied ones would have to be set to obtain homogeneity for the $DME + C_5 + PB + H_2$ system. Such a choice would however imply higher pressures at a given temperature.

Fig. 12 shows three different isochores at increasing hydrogen content of the mixture at a given density. The ratio between the number of moles of hydrogen and the number of moles of double bonds present in the polymer increases from 10:1 (violet circles) to 15:1 (blue circles) and to 20:1 (triangles). Comparing these three isochores it is concluded that the higher the H_2 / PB ratio, the higher the pressure of the quaternary mixture. This conclusion is important in relation to the initial conditions for the hydrogenation reaction.

No observable degradation (decrease of average molecular weights Mn and Mw) of the polymer was observed, as confirmed by looking at the SEC chromatogram of PB before and after the measurements in the cell.

5. Remarks and conclusions

Using a constant volume equilibrium cell, isochoric/isoplethic pressure versus temperature trajectories were experimen-

tally studied for pure compounds (CO_2 and toluene), and for binary ($DME + C_5$), ternary ($DME + C_5 + PB$) and quaternary ($DME + C_5 + PB + H_2$) mixtures. This experimental information is important in the context of the potential hydrogenation of PB under fluid homogeneity conditions. The experimental results will guide us in the selection of the optimal conditions (composition of the initial reactive mixture, temperature and global density) to carry out the PB hydrogenation in batch mode, using $DME + C_5$ as the binary solvent mixture.

The experimental results show that the homogeneous-liquid isochoric pressure-temperature coefficient (P vs. T slope) decreases with the decrease in the global density at constant overall composition (e.g., Fig. 5) for pure compounds, binary and ternary mixtures.

In the case of ternary mixtures, the slope in the homogeneous region at constant overall density (see Fig. 8) does not show a clear change when w_{C5} changes. For quaternary mixtures, at a given temperature and density, a higher H_2 / PB ratio implies a higher pressure (see Fig. 12).

The PC-SAFT EoS was used to model the phase behavior of pure compounds, and of binary and ternary mixtures. We computed isoplethic/isochoric loci and phase envelopes, achieving, in general terms, an acceptable level of agreement with the experimental data.
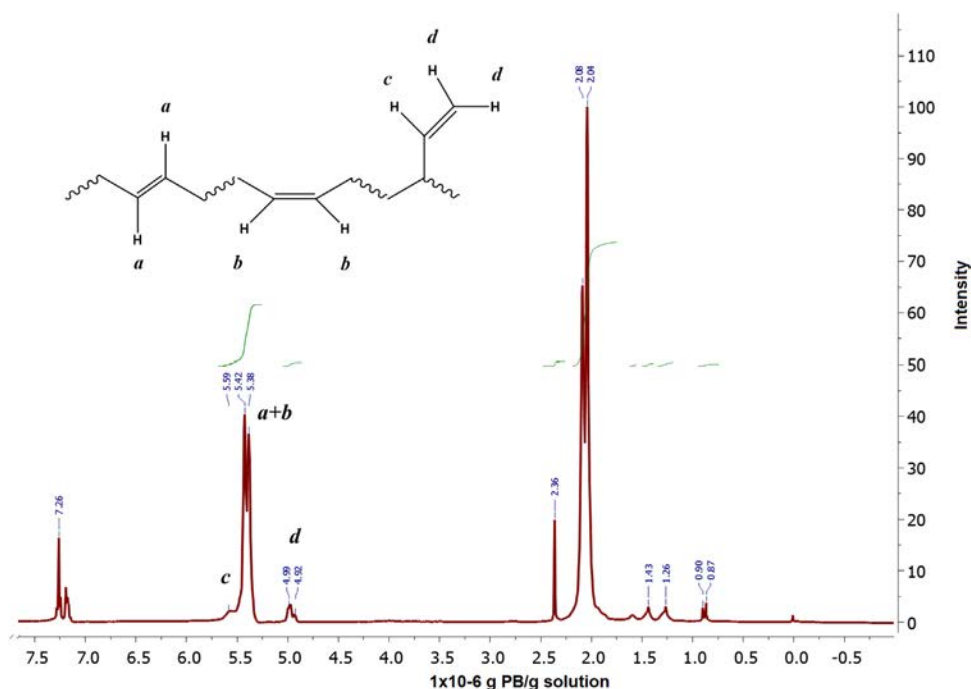
Declaration of Competing Interest

None.

Appendix A. ^{1}H NMR spectrum of polybutadiene

References

[1] C.M. Piqueras, G. Tonetto, S. Bottini, D.E. Damiani, Sunflower oil hydrogenation on Pt catalysts: comparison between conventional process and homogeneous phase operation using supercritical propane, Catal. Today 133–135 (2008) 836–841, http://dx.doi.org/10.1016/j.cattod.2007.11.036.

[2] J.M. Milanesio, G.D.B. Mabe, A.E. Ciolino, L.M. Quinzani, M.S. Zabaloy, Experimental cloud points for polybutadiene + light solvent and polyethylene + light solvent systems at high pressure, J. Supercrit. Fluids 55 (2010) 363–372, http://dx.doi.org/10.1016/j.supflu.2010.07.011.

[3] J.T. Gotro, W.W. Graessley, Model hydrocarbon polymers - rheological properties of linear polyisoprenes and hydrogenated polyisoprenes, Macromolecules 17 (1984) 2767–2775, http://dx.doi.org/10.1021/ma00142a058.

[4] G.A. Cassano, E.M. Vallés, L.M. Quinzani, Structure of partially hydrogenated polybutadienes, Polymer 39 (1998) 5573–5577, http://dx.doi.org/10.1016/S0032-3861(97)10080-5.

[5] H.G.M. Edwards, D.W. Farwell, A.F. Johnson, I.R. Lewis, N. Webb, N.J. Ward, Spectroscopic studies of an ambient-pressure process for the selective hydrogenation of polybutadienes, Macromolecules 25 (1992) 525–529, http://dx.doi.org/10.1021/ma00028a005.

[6] J.S. Parent, N.T. Mcmanus, G.L. Rempel, RhCl(PPh3)3 and RhH(PPh3)4 catalyzed hydrogenation of acrylonitrile-butadiene copolymers, Ind. Eng. Chem. Res. 35 (1996) 4417–4423, http://dx.doi.org/10.1021/ie9506680.

[7] N. Andreucetti, J. Pérez, M. Failla, E. Vallés, Modification of model ethylene-butene copolymers using gamma radiation and an organic peroxide, Macromol. Symp. 245–246 (2006) 93–105, http://dx.doi.org/10.1002/masy.200651313.

[8] J.M. Milanesio, G.D.B. Mabe, A.E. Ciolino, L.M. Quinzani, M.S. Zabaloy, High-pressure liquid–liquid equilibrium boundaries for systems containing polybutadiene and/or polyethylene and a light solvent or solvent mixture, J. Supercrit. Fluids 72 (2012) 333–339, http://dx.doi.org/10.1016/j.supflu.2012.10.007.

[9] L. Yurttaş, J.C. Holste, K.R. Hall, B.E. Gammon, K.N. Marsh, Semiautomated isochoric apparatus for p-V-T and phase equilibrium studies, J. Chem. Eng. Data 39 (1994) 418–423, http://dx.doi.org/10.1021/je00015a004.

[10] J. Zhou, P. Patil, S. Ejaz, M. Atilhan, J.C. Holste, K.R. Hall, (P, Vm, T) and phase equilibrium measurements for a natural gas-like mixture using an automated isochoric apparatus, J. Chem. Thermodyn. 38 (2006) 1489–1494, http://dx.doi.org/10.1016/j.jct.2005.12.011.

[11] A. Velez, S. Pereda, E.A. Brignole, Isochoric lines and determination of phase transitions in supercritical reactors, J. Supercrit. Fluids 55 (2010) 643–657, http://dx.doi.org/10.1016/j.supflu.2010.09.033.

[12] A. Velez, P. Hegel, G.D.B. Mabe, E.A. Brignole, Density and conversion in biodiesel production with supercritical methanol, Ind. Eng. Chem. Res. 49 (2010) 7666–7670, http://dx.doi.org/10.1021/ie100670r.

[13] M. Atilhan, J. Zhou, S. Ejaz, D. Cristancho, J. Holste, K.R. Hall, Phase behavior concerns for multicomponent natural gas-like mixtures, in: Proceedings of the 1st Annual Gas Processing Symposium, Elvesier, Doha, 2009.

[14] DIPPR-801, Evaluated Process Design Data, Public Release. American Institute of Chemical Engineers, Design Institute for Physical Property Data, BYU-DIPPR, Thermophysical Properties Laboratory, Provo, Utah, 2003.

[15] M. Morton, Anionic Polymerization: Principles and Practice, Academic Press. Inc., New York, 1983.

[16] J. Brandrup, E.H. Immergut, E.A. Grulk, Polymer Handbook, Wiley, New York, 1999.

[17] Q. Gao, Y. Wang, Y. Ren, Y. Li, Facile synthesis of amphiphilic heterografted copolymers with crystalline and amorphous side chains, Macromol. Chem. Phys. 214 (2013) 1677–1687, http://dx.doi.org/10.1002/macp.201300255.

[18] S.B. Rodriguez-Reartes, M. Cismondi, E. Franceschi, M.L. Corazza, J.V. Oliveira, M.S. Zabaloy, High-pressure phase equilibria of systems carbon dioxide + n-eicosane and propane + n-eicosane, J. Supercrit. Fluids 50 (2009) 193–202, http://dx.doi.org/10.1016/j.supflu.2009.06.017.

[19] Eric W. Lemmon, Mark O. McLinden, Daniel G. Friend, in: P.J. Linstrom, W.G. Mallard (Eds.), Thermophysical Properties of Fluid Systems NIST Chemistry WebBook, NIST Standard Reference Database Number 69, National Institute of Standards and Technology, Gaithersburg MD, 2019, p. 20899, http://dx.doi.org/10.18434/T4D303 (May 15th, 2019).

[20] J. Gross, G. Sadowski, Perturbed-chain SAFT: an equation of state based on a perturbation theory for chain molecules, Ind. Eng. Chem. Res. 40 (2001) 1244–1260, http://dx.doi.org/10.1021/ie0003887.

[21] E.C. Ihmels, E.W. Lemmon, Experimental densities, vapor pressures, and critical point, and a fundamental equation of state for dimethyl ether, Fluid Phase Equilib. 260 (2007) 36–48, http://dx.doi.org/10.1016/j.fluid.2006.09.016.

[22] M. Cismondi, M.L. Michelsen, Global phase equilibrium calculations: critical lines, critical end points and liquid-liquid-vapour equilibrium in binary mixtures, J. Supercrit. Fluids 39 (2007) 287–295, http://dx.doi.org/10.1016/j.supflu.2006.03.011.

[23] S.L. Outcalt, E.W. Lemmon, Density measurements of compressed-liquid dimethyl ether + pentane mixtures, High Temp. - High Press. 45 (2016) 21–33.

[24] S.L. Outcalt, E.W. Lemmon, Bubble-point measurements of eight binary mixtures for organic Rankine cycle applications, J. Chem. Eng. Data 58 (2013) 1853–1860, http://dx.doi.org/10.1021/je400251s.

[25] L. Yelash, M. Müller, P. Wolfgang, K. Binder, Artificial multiple criticality and phase equilibria: an investigation of the PC-SAFT approach, Phys. Chem. Chem. Phys. 7 (2005) 3728–3732, http://dx.doi.org/10.1039/b509101m.

[26] H.S. Byun, D.H. Lee, Phase behavior of binary and ternary mixtures of poly(decyl acrylate)-supercritical solvents-decyl acrylate and poly(decyl methacrylate)-CO2-decyl methacrylate systems, Ind. Eng. Chem. Res. 45 (2006) 3373–3380, http://dx.doi.org/10.1021/ie0507070.